

# Optical and magneto-optical FIR properties of bilayer graphene

D.S.L. Abergel and Vladimir I. Fal'ko  
*Physics Department, Lancaster University, Lancaster, LA1 4YB, UK*

We analyse spectroscopic features of bilayer graphene in comparison to the monolayer material. We show how the formation of pairs of low-energy and split bands in a bilayer is manifested in its optical absorption. We also show that the inter-Landau-level absorption in bilayer graphene at a high magnetic field is much denser in the FIR range than that in monolayer material, and that the polarisation dependence of its lowest energy peak can be used to test the form of the bilayer ground state in the quantum Hall effect regime.

Graphene (atomic mono- and bilayer of graphite) [1, 2, 3] is a gapless two-dimensional (2D) semiconductor [5, 6]. When used in transistor-type devices, the density and type (*n* or *p*) of carriers in it can be controlled using the underlying gate [1], which has been exploited in the recent studies of the quantum Hall effect (QHE) in such structures. The sequencing of QHE plateaux in graphene [1, 2, 3] revealed peculiar properties of charge carriers in this material: Dirac-type chiral electrons with Berry phase  $\pi$  in monolayers [4, 5] and a new type of chiral quasiparticles [6] with Berry phase  $2\pi$  and doubled degeneracy of the zero-energy Landau level (LL) in bilayers.

The microwave absorption in monolayer graphene has been discussed in recent literature [7, 8, 9]. While the DC conductivity of monolayer graphene increases linearly with the carrier density [1, 10], the real part of its high-frequency conductivity is independent of the electron density in a wide spectral range above the threshold  $\hbar\omega > 2|\epsilon_F|$ , which determines a constant coefficient  $g_1 = \pi e^2/2\hbar c$  of absorption of electromagnetic (EM) field. In this Letter we propose a theory for the optical and far-infrared (FIR) properties of bilayer graphene. We calculate the bilayer absorption coefficient,

$$g_2 = (\pi e^2/\hbar c) f_2(\omega), \quad (1)$$

and show how in contrast to a featureless  $g_1$  in a monolayer [7, 8],  $g_2$  reflects the bilayer band structure, as shown in Fig.1. Then we compare the far-infrared (FIR) absorption spectrum of bilayer and monolayer graphene in a strong magnetic field (due to the inter-LL [6, 11] transitions), show that it is much denser in bilayer than in monolayer material, and investigate its dependence on the polarisation of the FIR irradiation.

The electronic Fermi line in graphene surrounds the corners [12]  $\mathbf{K}_\pm$  of the hexagonal Brillouin zone [5] (where we set  $\epsilon = 0$ ). In monolayer graphene, quasiparticles near the centres of valleys  $\mathbf{K}_\pm$  can be described by 4-component Bloch functions  $\psi = [\phi_{\mathbf{K}_+A}, \phi_{\mathbf{K}_+B}, \phi_{\mathbf{K}_-B}, \phi_{\mathbf{K}_-A}]$  and the Hamiltonian  $\hat{H}_1 = \xi v \sigma \cdot \mathbf{p}$ , where  $\sigma = (\sigma_x, \sigma_y)$  are Pauli matrices acting in the space of electronic amplitudes on the two crystalline sublattices (*A* and *B*),  $\xi = \pm$  in  $\mathbf{K}_\pm$  distinguishes between valleys, momentum  $\mathbf{p} = -i\hbar\nabla - \frac{e}{c}\mathbf{A}$  is calculated with respect to

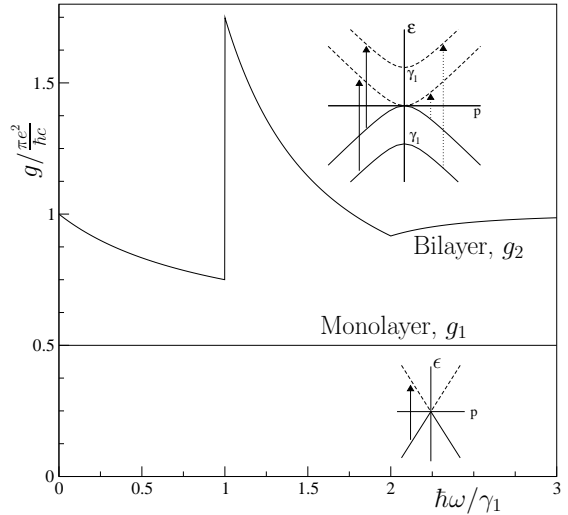


FIG. 1: Absorption coefficient of bilayer and monolayer graphene in the optical range of frequencies. Insets illustrate the quasiparticle dispersion branches in the vicinity of  $\epsilon_F$  and possible optical transitions.

the center of the corresponding valley and  $\nabla \times \mathbf{A} = B\mathbf{l}_z$ .

*Bilayer graphene* is composed of two coupled monolayers (with sublattices *A*, *B* and  $\tilde{A}$ ,  $\tilde{B}$  in the bottom and top layer respectively) arranged according to Bernal stacking [5]: sites *B* of the honeycomb lattice in the bottom layer lie below  $\tilde{A}$  of the top layer. It also has a hexagonal Brillouin zone with two inequivalent valleys, but carries twice the number of electronic dispersion branches which can be found using the next-neighbour hopping Hamiltonian [6] acting in the space of sublattice states  $[\phi_{\mathbf{K}_+A}, \phi_{\mathbf{K}_+\tilde{B}}, \phi_{\mathbf{K}_+\tilde{A}}, \phi_{\mathbf{K}_+B}; \phi_{\mathbf{K}_-A}, \phi_{\mathbf{K}_-\tilde{B}}, \phi_{\mathbf{K}_-\tilde{A}}, \phi_{\mathbf{K}_-B}]$ ,

$$\hat{H}_2 \approx \begin{pmatrix} \xi v_3 \sigma^t \cdot \mathbf{p} & \xi v \sigma \cdot \mathbf{p} \\ \xi v \sigma \cdot \mathbf{p} & \gamma_1 \sigma_x \end{pmatrix}. \quad (2)$$

Here,  $v$  is determined by the *AB* ( $\tilde{A}\tilde{B}$ ) intra-layer hopping,  $\gamma_1$  is the strongest inter-layer  $\tilde{A}\tilde{B}$  hopping element, and  $v_3 \ll v$  is due to a direct weak hop between  $A\tilde{B}$  sublattices. Note that  $\sigma_{x,y,z}^t$  are transposed matrices. Equation (2) determines two types of branches in the electronic spectrum of graphene [6, 13] observed in the

recent ARPES studies [14]: split-bands,

$$\varepsilon_s^\pm = \pm(\gamma_1/2)[\sqrt{1+4v^2p^2/\gamma_1^2} + 1], \quad (3)$$

formed by symmetric and antisymmetric states based upon  $\tilde{A}\tilde{B}$  sublattices and two the gapless branches,  $\varepsilon_c^\pm$ . For  $\epsilon \gg \epsilon_L \equiv \frac{1}{2}\gamma_1(v_3/v)^2$ , the dispersion in gapless branches can be approximated by

$$\varepsilon_c^\pm = \pm(\gamma_1/2)[\sqrt{1+4v^2p^2/\gamma_1^2} - 1]. \quad (4)$$

For  $|\epsilon| < \frac{1}{4}\gamma_1$ , gapless bands are formed by states from sublattices  $A$  and  $\tilde{B}$  described using the 4-component Bloch functions  $\chi = [\phi_{\mathbf{K}+A}, \phi_{\mathbf{K}+\tilde{B}}, \phi_{\mathbf{K}-\tilde{B}}, \phi_{\mathbf{K}-A}]$  and the reduced low-energy Hamiltonian [6, 15],

$$\begin{aligned} \hat{H}_2 &= -\frac{1}{2m_2}(\sigma \cdot \mathbf{p})\sigma_x(\sigma \cdot \mathbf{p}) + \delta\hat{H}_w + \frac{\beta p^2}{m_2}; \quad (5) \\ \delta\hat{H}_w &= \xi v_3 \sigma^t \cdot \mathbf{p}; \quad m_2 = \gamma_1/2v^2, \quad |\beta| \ll 1. \end{aligned}$$

Here  $m_2 \approx 0.055m_e$  and the last term in  $\hat{H}_2$  takes into account the weak  $AA$  and  $BB$  intra-layer hopping [16].

In a 2D electron gas with conductivity  $\sigma(\omega) \ll c/2\pi$ , absorption of an EM field  $\mathbf{E}_\omega = \ell E e^{-i\omega t}$  with polarisation  $\ell$  [ $\ell_{\oplus/\ominus} = [l_x \pm il_y]/\sqrt{2}$  describe right(+) and left(−) hand circularly polarised light] can be characterised by the absorption coefficient  $g \equiv E_i E_j^* \sigma_{ij}(\omega)/S$ : the ratio between Joule heating and the energy flux  $\mathbf{S} = c\mathbf{E} \times \mathbf{H}/4\pi = S\mathbf{l}_z$  transported by the EM field. Using the Keldysh technique, we express

$$g = \frac{4\pi e^2}{c\omega} \Re \int \frac{F d\epsilon}{2\pi N} \widehat{\text{Tr}} \left\{ \hat{v}_i \ell_i \hat{G}^R(\epsilon) \hat{v}_j \ell_j^* \hat{G}^A(\epsilon + \omega) \right\},$$

where  $\hat{v} = \partial_{\mathbf{p}} \hat{H}$  is velocity operator,  $\widehat{\text{Tr}}$  includes the summation both over the sublattice indices “tr” and over single-particle orbital states,  $N$  is the normalisation area of the sample and  $F = n_F(\epsilon) - n_F(\epsilon + \omega)$  takes into account the occupancy of the initial and final states.

*Optical properties of bilayer graphene at zero magnetic field.* For a 2D gas in a zero magnetic field, the electron states are weakly scattered plane waves. Using the plane wave basis and the matrix form of the bilayer Hamiltonian  $\hat{H}_2$ , we express the retarded/advanced Green functions of electrons in the bilayer as  $\hat{G}^{R/A}(\mathbf{p}, \epsilon) = [\epsilon \pm \frac{1}{2}i\hbar\tau^{-1} - \hat{H}_2(\mathbf{p})]^{-1}$  and  $\widehat{\text{Tr}} = \int d^2\mathbf{p} \frac{N}{(2\pi\hbar)^2} \text{tr}$ . After neglecting the renormalisation of the current operator by vertex corrections at  $\omega\tau \gg 1$  and the momentum transfer from light (since  $v/c \sim 3 \times 10^{-3}$ ), we reproduce [7, 8] the constant absorption coefficient  $g_1^{\parallel} = \pi e^2/2\hbar c$  ( $f_1 = \frac{1}{2}$ ) in monolayer graphene and arrive at the expression for the absorption coefficient of a bilayer for light polarised in the plane of graphene sheet [19]:

$$\begin{aligned} g_2^{\parallel} &= \frac{\pi e^2}{\hbar c} f_2(\Omega), \quad \Omega \equiv \frac{\hbar\omega}{\gamma_1} > \frac{2|\epsilon_F|}{\gamma_1}, \quad (6) \\ f_2 &= \frac{\Omega + 2}{2(\Omega + 1)} + \frac{\theta(\Omega - 1)}{\Omega^2} + \frac{(\Omega - 2)\theta(\Omega - 2)}{2(\Omega - 1)}, \end{aligned}$$

where  $\theta(x < 0) = 0$  and  $\theta(x > 0) = 1$ . In the limit of intermediate frequencies  $\hbar\omega \ll \frac{1}{4}\gamma_1$  this result transforms into  $f(\Omega \ll 1) = 1$  suggested by J.Cserti [17] for the description of microwave absorption in bilayer graphene. However one should be aware that Eq. (6) and conclusions of Ref. [17] cannot be applied to frequencies  $\hbar\omega \lesssim \epsilon_L = \frac{1}{2}\gamma_1(v_3/v)^2 \sim 1\text{meV}$ , where the warping term  $\delta\hat{H}_w$  in the bilayer Hamiltonian starts playing an important role [6]. At  $\epsilon_F \approx \epsilon_L$ ,  $\delta\hat{H}_w$  causes the Lifshitz transition [18] in the topology of the Fermi line of 2D electrons: four pockets (in each valley) at  $\epsilon_F < \epsilon_L$  become a singly-connected Fermi line at  $\epsilon_F > \epsilon_L$ .

The frequency dependence of the bilayer optical absorption is illustrated in Fig.1, where an additional structure in the vicinity of  $\hbar\omega = \gamma_1$  ( $\gamma_1 \approx 0.4\text{eV}$  [5, 14]) is due to the electron-hole excitation between the low-energy band  $\varepsilon_c^\pm$  and the split band  $\varepsilon_s^\pm$ . For the higher photon energies,  $\hbar\omega \gtrsim 2\gamma_1$ , the frequency dependence almost saturates at  $f \approx 1$ . Over the entire spectral interval shown in Fig.1, the absorption coefficient for the left- and right-handed light are the same, so that Eq. (6) is applicable [19] to light linearly polarised in the graphene plane.

*High-field FIR magneto-optics of graphene.* In a strong magnetic field the spectrum of 2D electrons consists of Landau levels (LLs). These can be evaluated after rewriting  $\hat{H}_1$  and  $\hat{H}_2$  in terms of descending,  $\pi = p_x + ip_y$  and raising,  $\pi^\dagger = p_x - ip_y$  operators in the basis of Landau functions  $\varphi_{n \geq 0}$ , leading to  $\sigma \cdot \mathbf{p} = \begin{pmatrix} 0 & \pi^\dagger \\ \pi & 0 \end{pmatrix}$ . The resulting monolayer spectrum [11] contains 4-fold degenerate (2× spin and 2× the valley index) states: one at  $\epsilon_0 = 0$  with  $\psi_{0K_+} = [\varphi_0, 0, 0, 0]$  and  $\psi_{0K_-} = [0, 0, \varphi_0, 0]$ , and pairs of levels  $\epsilon_{n\pm} = \pm\hbar v \lambda_B^{-1} \sqrt{2n}$  ( $\lambda_B = \sqrt{\hbar c/eB}$  is the magnetic length) with  $\psi_{n\pm, K_+} = \frac{1}{\sqrt{2}}[\varphi_n, \mp i\varphi_{n-1}, 0, 0]$  and  $\psi_{n\pm, K_-} = \frac{1}{\sqrt{2}}[0, 0, \varphi_n, \mp i\varphi_{n-1}]$ . We neglect the electron spin splitting and use the index  $\alpha = \pm$  in  $\epsilon_{n\alpha}$  and  $\psi_{n\alpha, K}$  for the conduction (+) and valence (−) band LLs.

The bilayer spectrum features [6] a group of 8 states with  $\epsilon_0 \approx \epsilon_1 \approx 0$ :  $\chi_{0K_+} = [\varphi_0, 0, 0, 0]$ ,  $\chi_{0K_-} = [0, 0, \varphi_0, 0]$  and  $\chi_{1K_+} = [\varphi_1, 0, 0, 0]$ ,  $\chi_{1K_-} = [0, 0, \varphi_1, 0]$  (4×2, due to spin degeneracy), and a ladder of almost equidistant 4-fold degenerate levels  $\epsilon_{n\pm} = \pm\hbar\omega_c \sqrt{n(n-1)}$  (2× spin and 2× the valley index) with  $\hbar\omega_c = \hbar^2/m_2 \lambda_B^2$  and wave functions  $\chi_{n\pm, K_+} = \frac{1}{\sqrt{2}}[\varphi_n, \pm i\varphi_{n-2}, 0, 0]$ ,  $\chi_{n\pm, K_-} = \frac{1}{\sqrt{2}}[0, 0, \varphi_n, \pm i\varphi_{n-2}]$ . The latter result can be found from the analysis of the first term in the low-energy-band Hamiltonian  $\hat{H}_2$ , which dominates for  $|\epsilon| < \frac{1}{4}\gamma_1$  and high magnetic fields such that  $\lambda_B^{-1} > \gamma_1 v_3/v^2$ . Numerical diagonalisation of the full  $\hat{H}_2$  and  $\hat{H}_2$  shows [6] that this degeneracy is not lifted by the warping term  $\delta\hat{H}_w$ , and also the above-described grouping of LLs in bilayer graphene was confirmed in the recent QHE measurements [3]. It has been noticed [15] that degenerate levels with  $n = 0$  ( $\chi_{0K_+}, \chi_{0K_-}$ ) and  $n = 1$  ( $\chi_{1K_+}, \chi_{1K_-}$ ) can be weakly split by the second-

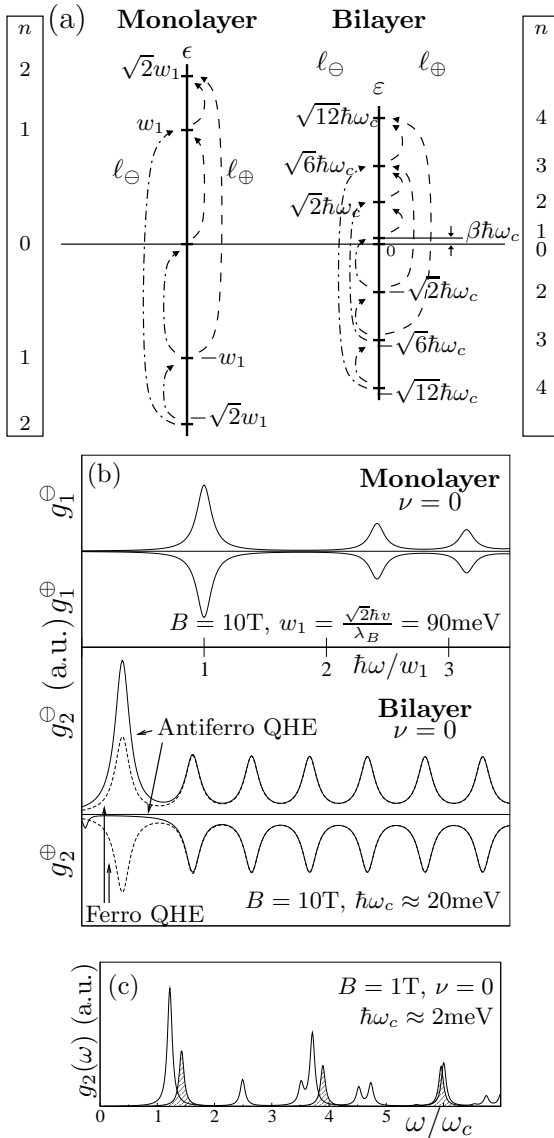


FIG. 2: (a) Allowed inter-LL transitions without trigonal warping effects. Dashed and dash-dot lines indicate transitions in  $\ell_{\oplus}$  and  $\ell_{\ominus}$  polarisations respectively. (b) Monolayer (top) and bilayer (bottom) FIR absorption spectra in  $\ell_{\oplus}$  and  $\ell_{\ominus}$  polarisations for  $B = 10T$  and filling factor  $\nu = 0$ . Dashed and solid lines describe absorption by ferro- and antiferromagnetic states of the  $\nu = 0$  bilayer. (c) Weak field,  $B = 1T$  magnetoabsorption in bilayer graphene with  $\nu = 0$  calculated with ( $v_3 = 0.2v$ ) and without ( $v_3 = 0$ , shaded) warping term in the Hamiltonian.

neighbour hopping term  $\beta p^2/m_2$ , to  $\epsilon_0 = \frac{\beta}{2}\hbar\omega_c$  and  $\epsilon_1 = \frac{3\beta}{2}\hbar\omega_c$ , where  $\beta \ll 1$  [16]. However, it is more likely that, at a high magnetic field, electrons in an ideally clean bilayer with filling factor  $-4 < \nu < 4$  would form a correlated ground state in which the occupancy of  $n = 0$  and 1 LLs would be determined by the electron-electron interaction. The correlated ground state is particularly interesting in a bilayer with  $\nu = 0$ , where 2D electrons

can form a ferromagnetic QHE state in which both  $n = 0$  and 1 states are half-filled, or an antiferromagnetic state with one fully occupied and one empty LL. Below we show that these two ground states can be distinguished experimentally on the basis of magneto-absorption spectra measured in a circularly polarised FIR light.

Figure 2(a) illustrates selection rules for the inter-LL transitions in bilayer and monolayer graphene. In both cases, photons with the in-plane [19] polarisation  $\ell_{\ominus}$  are absorbed via transitions where the LL index changes as  $n \rightarrow n - 1$  ( $n \geq 1$ ), whereas absorption of  $\ell_{\oplus}$  photons happens via transitions  $n \rightarrow n + 1$  ( $n \geq 0$ ). Assuming the same broadening  $\hbar\tau^{-1}$  of all LLs [20], we arrive at the following magneto-absorption spectra for monolayer [9] and bilayer graphene (for  $\epsilon_{\text{L}} < \hbar\omega < \frac{1}{4}\gamma_1$ ):

$$g_J^{\oplus/\ominus}(B, \omega) = \frac{\pi e^2}{\hbar c} f_J^{\oplus/\ominus}(B, \omega), \quad (7)$$

$$f_1^{\ominus} = \sum_{n \geq 1} \frac{\frac{w_1 \tau}{\pi \hbar} \frac{b_{n-1}^2}{\alpha \sqrt{n-1} - \alpha' \sqrt{n}} (\nu_{n,\alpha'} - \nu_{n-1,\alpha})}{\frac{w_1^2 \tau^2}{\hbar^2} [\frac{\hbar\omega}{w_1} - \alpha \sqrt{n-1} + \alpha' \sqrt{n}]^2 + 1}$$

$$f_1^{\oplus} = \sum_{n \geq 0} \frac{\frac{w_1 \tau}{\pi \hbar} \frac{b_n^2}{\alpha \sqrt{n+1} - \alpha' \sqrt{n}} (\nu_{n,\alpha'} - \nu_{n+1,\alpha})}{\frac{w_1^2 \tau^2}{\hbar^2} [\frac{\hbar\omega}{w_1} - \alpha \sqrt{n+1} + \alpha' \sqrt{n}]^2 + 1}$$

$$f_2^{\ominus} = \sum_{n \geq 2} \frac{\frac{2c_{n-1}^2}{\pi \omega_c \tau} \frac{(\nu_{n,\alpha'} - \nu_{n-1,\alpha})(n-1)}{\alpha \sqrt{n^2 - n} - \alpha' \sqrt{(n-1)(n-2)}}}{[\frac{\omega}{\omega_c} - \alpha \sqrt{n^2 - n} + \alpha' \sqrt{(n-1)(n-2)}]^2 + \frac{\tau^{-2}}{\omega_c^2}}$$

$$f_2^{\oplus} = \sum_{n \geq 1} \frac{\frac{2c_n^2}{\pi \omega_c \tau} \frac{(\nu_{n,\alpha'} - \nu_{n+1,\alpha})n}{\alpha \sqrt{n^2 + n} - \alpha' \sqrt{n^2 - n}}}{[\frac{\omega}{\omega_c} - \alpha \sqrt{n^2 + n} + \alpha' \sqrt{n^2 - n}]^2 + \frac{\tau^{-2}}{\omega_c^2}}.$$

Here  $w_1 = \sqrt{2}\hbar v \lambda_B^{-1}$  and  $\hbar\omega_c = \hbar^2/m_2 \lambda_B^2$  are the characteristic energy scales for the LL spectra in monolayer ( $J = 1; \epsilon_{n\alpha}$ ) and bilayer ( $J = 2; \epsilon_{n\alpha}$ ) graphene, respectively, and  $\alpha, \alpha' = \pm$  determine whether the corresponding state belongs to the conduction (+) or valence (--) band. Also,  $\nu_{n,\alpha}$  are the filling factors of the corresponding LLs, and  $b_0 = 1$ ,  $b_{n \geq 1} = 1/\sqrt{2}$  for a monolayer and  $c_{0,1} = 1$ ,  $c_{n \geq 2} = 1/\sqrt{2}$  for the bilayer.

The denser magneto-absorption spectrum in bilayer graphene (as compared to the monolayer) is one of its features illustrated in Fig. 2(b). Another feature is that the intensity of the lowest absorption peak measured at the filling factor  $\nu = 0$  may differ for  $\ell_{\oplus}$  and  $\ell_{\ominus}$  polarisations, reflecting the form of the ground state of a bilayer. Since transitions from/to the  $n = 0$  LL with  $\epsilon_0 \approx 0$  to/from the states  $\epsilon_{n\pm}$  with  $n \geq 2$  are forbidden, the intensity and polarisation of the peak at  $\omega = \sqrt{2}\hbar\omega_c$  are determined by transitions from/to  $n = 1$  LL (also with  $\epsilon_1 \approx 0$ ) and directly reflect its occupancy. If the bilayer ground state is ferromagnetic, with a half-filled  $n = 1$  LL, the absorption peak at  $\omega = \sqrt{2}\hbar\omega_c$  will have the same intensity in both  $\ell_{\oplus}$  and  $\ell_{\ominus}$  polarisations. In contrast, absorption

by a  $\nu = 0$  bilayer with antiferromagnetic ground state would contain this line only in one polarisation: in  $\ell_\ominus$  if  $n = 1$  LL is empty (fully occupied  $n = 0$  LL) and in  $\ell_\oplus$  if  $n = 1$  LL is full. For comparison, the lowest peak in the spectrum of a monolayer with  $\nu = 0$  appears in both polarisations, since both transitions to  $(\epsilon_{1-} \rightarrow \epsilon_0)$  and from  $(\epsilon_0 \rightarrow \epsilon_{1+})$  half-filled  $n = 0$  monolayer LL are possible. All higher-energy absorption peaks which involve transitions between filled valence band states ( $\alpha = -$ ) and empty states in the conduction band ( $\alpha = +$ ) have equal strengths in both polarisations.

One can test the selection rules shown in Fig. 2(a) using gated graphene structures [1, 2, 3]. By filling the monolayer sheet with electrons up to  $\nu = 2$  (a completely filled  $n = 0$  LL), one would suppress the intensity of the lowest absorption peak in  $\ell_\ominus$  polarisation and double its size in the polarisation  $\ell_\oplus$ . By depleting the monolayer to  $\nu = -2$  state (emptying the  $n = 0$  LL) one would achieve the opposite effect. Similarly, in a bilayer with a completely filled pair of degenerate  $\epsilon_0 \approx \epsilon_1 \approx 0$  LLs which takes place at  $\nu = 4$ , light with  $\omega = \sqrt{2}\omega_c$  can be absorbed only in the  $\ell_\oplus$  polarisation. By depleting the bilayer down to  $\nu = -4$  one could suppress the absorption in this line in  $\ell_\oplus$  polarisation while retaining  $\ell_\ominus$  absorption. Also, note that a weak transition between  $n = 0$  and 1 LLs with a low frequency  $\beta\omega_c$  (microwave range) is possible, to the measure of a small  $\beta$  and depending on the LL filling.

Finally, the warping term  $\delta\hat{H}_w$  in Eq. (5) mixes each state  $\chi_{n\alpha,K}$  with states  $\chi_{(n\pm 3)\alpha,K}$ . This generates weak transitions (with the coefficient  $\delta g_2 \sim (v_3 m_2 \lambda_B/\hbar)^2 g_2$ ) between states which are 2 and 4 levels apart. Although such transitions are negligibly weak at high fields where the first term in  $\hat{H}_2$  is dominant, they become relevant at weak fields, where  $\lambda_B^{-1} \lesssim \gamma_1 v_3/v^2$ , and the low-frequency absorption spectrum of a bilayer acquires an additional structure. In Fig.2(c) we compare the absorption spectra in a  $\nu = 0$  bilayer [20] at  $B = 1$ T calculated numerically for  $v_3 = 0$  and  $v_3 = 0.2v$ .

In conclusion, we have described peculiar optical and FIR magneto-optical properties of bilayer graphene. The optical absorption spectrum shown in Fig.1 for the frequency range  $\hbar\omega \lesssim 3\gamma_1$  reflects the existance of four bands in the electronic spectrum of this material and demonstrates that in the visible spectral range (photon energies  $\hbar\omega \gtrsim 2\gamma_1$ ) the bilayer absorption coefficient,  $g_2 \approx \pi e^2/\hbar c \approx 2.3 \times 10^{-2}$  is twice larger than that in a monolayer. Also, we showed that the FIR magneto-optical spectrum of bilayer graphene is much denser than that of a monolayer, reflecting the parabolic dispersion of its low-energy bands  $\epsilon_c^\pm$ . We also suggested that the polarisation dependence of the lowest FIR absorption peak in a bilayer, at  $\omega = \sqrt{2}\omega_c$  can be used to determine the structure of its  $\nu = 0$  QHE ground state formed of two degenerate [6] zero-energy Landau levels,  $n = 0$  and  $n = 1$ .

In such spectroscopic studies, the weakness of  $g_2$  can be overcome using the transport detection of FIR absorption in the QHE regime.

We thank E.McCann and A.Varlamov for discussions and the EPSRC grant EP/C511743 for support.

---

[1] K. Novoselov *et al*, Nature **438**, 197 (2005); Science **306**, 666 (2004)

[2] Y. Zhang *et al*, Phys. Rev. Lett. **94**, 176803 (2005); Nature **438**, 201 (2005)

[3] K. Novoselov *et al*, Nature Physics **2**, 177 (2006)

[4] Y. Zheng, T. Ando, Phys. Rev. B **65**, 245420 (2002); V. Gusynin, S. Sharapov, Phys. Rev. Lett. **95**, 146801 (2005); A. Castro Neto, F. Guinea, N. Peres, Phys. Rev. B **73**, 205408 (2006)

[5] M. S. Dresselhaus and G. Dresselhaus, Adv. Phys. **51**, 1 (2002); T. Ando, J. Phys. Soc. Jpn. **74**, 777 (2005)

[6] E. McCann and V.I. Fal'ko, Phys Rev. Lett. **96** 086805 (2006)

[7] V. Gusynin, S. Sharapov, J. Carbotte, Phys. Rev. Lett. **96**, 256802 (2006); V. Gusynin and S. Sharapov, Phys. Rev. B **73**, 245411 (2006)

[8] L. Falkovsky and A. Varlamov, cond-mat/0606800

[9] M. Sadowski *et al*, cond-mat/0605739; A. Iyengar *et al*, cond-mat/0608364

[10] K. Nomura and A.H. MacDonald, Phys. Rev. Lett. **96**, 256602 (2006); T. Ando, J. Phys. Soc. Jpn. **75**, 074716 (2006); V. Cheianov and V.I. Fal'ko, cond-mat/0608228

[11] J.W. McClure, Phys. Rev. **104**, 666 (1956)

[12] Here,  $\mathbf{K}_\pm = \pm(\frac{2}{3}ha^{-1}, 0)$ ,  $a$  is the lattice constant.

[13] C. Lu *et al*, Phys. Rev. B **73**, 144427 (2006); J. Nilsson *et al*, Phys. Rev. B **73**, 214418 (2006); M. Koshino, T. Ando, Phys. Rev. B **73**, 245403 (2006); F. Guinea, A. Castro Neto, N. Peres, Phys. Rev. B **73**, 245426 (2006); B. Partoens, F. Peeters, Phys. Rev. B **74**, 075404 (2006)

[14] T. Ohta *et al*, Science **313**, 951 (2006)

[15] E. McCann, Phys. Rev. B **74**, 161403 (2006)

[16] The sign of  $\beta$  is not known, though one can estimate using bulk graphite parameters [5] that  $|\beta| \lesssim 10^{-2}$ .

[17] J. Cserti, cond-mat/0608219

[18] A.A. Abrikosov, *Fundamentals of the Theory of Metals*, North-Holland 1988

[19] In contrast to monolayer graphene, a weak absorption of light polarised perpendicular to the bilayer is possible. A perturbation  $\sigma_z e E_z d/2$  distinguishes between the on-site energies in the top and bottom layers separated by spacing  $d$ , which leads to weak absorption  $g_2^z = (\pi e^2/\hbar c) f_2^z$ ,

$$f_2^z = \frac{1}{2} a_z^2 \Omega \left[ \frac{1}{\Omega+1} + \frac{\theta(\Omega-2)}{\Omega-1} \right], \quad \Omega \equiv \hbar\omega/\gamma_1;$$

$$f_2^z(B, \omega) = \frac{a_z^2}{2\pi} \sum_{n \geq 2} \frac{\tau\omega}{\tau^2 \omega_c^2 (\frac{\omega}{\omega_c} - 2\sqrt{n^2 - n})^2 + 1}$$

where  $a_z = \gamma_1 d/2\hbar v \sim 10^{-1}$ , and the magneto-absorption spectrum at  $\hbar\omega < \frac{1}{4}\gamma_1$  involves  $\epsilon_{n-} \rightarrow \epsilon_{n+}$  inter-LL transitions.

[20] For energy-dependent broadening one replaces  $\tau^{-1}$  in the sum in Eq. (7) with  $\tau_{n\alpha, n'\alpha'}^{-1} = \frac{1}{2}(\tau_{n\alpha}^{-1} + \tau_{n'\alpha'}^{-1})$ .